Dense Estimation of Surface Reflectance Properties Based on Inverse Global Illumination Rendering

Takashi Machida† , Haruo Takemura† and Naokazu Yokoya‡
†Cybermedia Center, Osaka University
‡Graduate School of Information Science, Nara Institute of Science and Technology
E-mail: {machida, takemura}@ime.cmc.osaka-u.ac.jp, yokoya@is.aist-nara.ac.jp

Abstract

In augmented virtuality, estimating object surface reflectance properties is important when rendering objects under arbitrary illumination conditions. However, faithfully estimating surface reflectance properties is difficult for objects having interreflections. The present paper describes a new method for densely estimating the non-uniform surface reflectance properties of real objects constructed of convex and concave surfaces having diffuse and specular interreflections. The registered range and surface color texture images were obtained using a laser rangefinder. In the proposed method, the light positions are first determined in order to take color images, which are then used to discriminate diffuse and specular reflection components of surface reflection. Surface reflectance parameters are then estimated based on an inverse global illumination rendering. Experiments were conducted to reveal the usefulness of the proposed method.

1 Introduction

In constructing a mixed reality (MR) environment, an inverse global illumination rendering is conducted in order to obtain the surface reflectance properties of virtualized real objects [2, 5]. For this purpose, we have studied the dense estimation of surface reflectance properties from range and surface texture images with diffuse interreflections [7]. In our previous research, an appropriate number of light positions are selected so that both diffuse and specular reflection components can be observed. Reflectance parameters can be then estimated. However, there remains a problem whereby specular interreflections cause errors.

Yu et al. [10] have estimated the surface reflectance properties of a room from color and geometry data considering both diffuse and specular interreflections based on inverse global illumination rendering. Boivin et al. [1] have also attempted to estimate surface reflectance properties considering diffuse interreflections. However, both of these methods assume that the surface of interest has uniform reflectance properties and therefore their algorithms cannot be applied to an non-uniform surface reflectance object.

In the present paper, we consider photon mapping [3], which is a global illumination rendering method. Photon mapping can represent diffuse and specular interreflections based on the emission of a photon from a light source. We propose herein a new method, using photon mapping, for estimating the non-uniform reflectance properties of objects with both diffuse and specular interreflections. In addition, the proposed method can densely estimate reflectance parameters by densely observing both reflection components.

2 Estimation of reflectance parameters from range and color images

Figure 1 shows a flow diagram of the estimation of surface reflectance properties. The proposed process consists of five procedures: measurement of the object (A,C), selection of a light source (B), initial estimation of reflectance parameters (D), and reflectance estimation via photon mapping (E).

2.1 Measurement and selection of light source positions

A laser rangefinder (Cyberware 3030RGB) along with known positions of a point light source and a camera are used to acquire surface color images, as illustrated in Figure 2(a). This system can obtain registered range and surface color texture images simultaneously by rotating the rangefinder and the camera around the object of interest.

In the present experimental setup, multiple positions of a light source are determined among 60 possible positions around the laser rangefinder, and these are two-

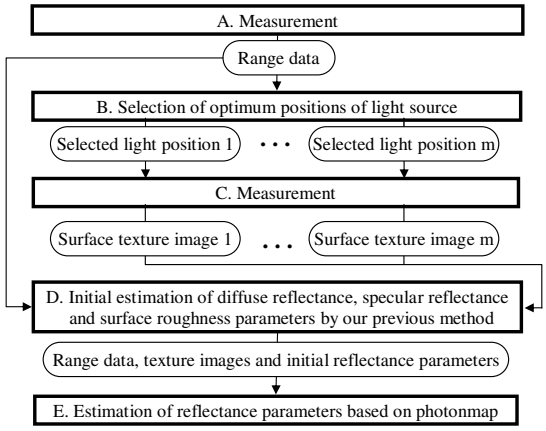

Figure 1. Flow diagram of estimating surface reflectance properties

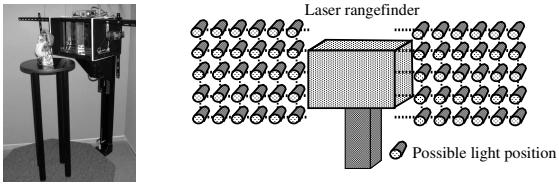

(a) Appearance of 3D-Digitizer

(b) Multiple possible light source positions

Figure 2. Experimental setup

dimensionally arranged at intervals of 5 cm, as shown in Figure 2(b). The positions of the camera and light source are calibrated in advance.

Here, we employ the Torrance-Sparrow model [8] to represent object reflectance properties physically. The Torrance-Sparrow model is given as:

$$i_x = \frac{Y}{D^2}\{P_{dx}\cos\theta_{dx} + \frac{P_{sx}}{\cos\theta_{vx}} exp(-\frac{\theta_{rx}^2}{2\sigma_x^2})\}, \quad (1)$$

where x denotes the surface point, i_x represents an observed intensity, D is an attenuation coefficient concerning the distance between a point light source and an object surface point, and Y represents the strength of a light source. P_{dx}, P_{sx} and σ_x are the diffuse reflectance, specular reflectance and surface roughness parameters, respectively. θ_{dx} is the angle between a light source vector and a surface normal vector, θ_{vx} is the angle between a viewing vector and a surface normal vector, and θ_{rx} is the angle between a viewing vector and a reflection vector. In order to densely estimate non-uniform reflectance parameters independently, optimum light positions for observing both reflection components at each surface point must be determined [6].

A texture image is obtained along with a selected light position p $(p = 1, \cdots, m)$ and consists of n pixels $(i_{p1}, \cdots, i_{pn})$, where i_{px} is the color intensity of a surface point x. Each pixel is classified as one of three types T_{diff}, T_{spec} or T_{none}. T_{diff} pixels contain only the diffuse reflection component and T_{spec} pixels contain a strong specular reflection component. T_{none} pixels are pixels that cannot be classified as neither T_{diff} or T_{spec}.

2.2 Estimation of reflectance parameters using photon mapping

As an initial estimation, the reflectance parameters are obtained using our previous method [6] in Figure 1(D). The diffuse reflectance parameter is estimated considering diffuse interreflections. The specular reflectance and the surface roughness parameters are estimated with no consideration of specular interreflections. Here, let P_{dx}^0, P_{sx}^0 and σ_x^0 be the reflectance parameters obtained in this process. These parameters are used as initial parameters for the next process (E) in Figure 1.

2.2.1 Photon mapping

In the photon mapping rendering method [3], an outgoing radiance L from a surface point x is calculated in order to decide a surface color. The following equations constitute the rendering equations in the photon mapping method.

$$L(x, \vec{\omega}) = L^e(x, \vec{\omega}) + L^r(x, \vec{\omega}), \quad (2)$$

$$L^r(x, \vec{\omega}) = \int_\Omega f(x, \vec{\omega}', \vec{\omega}) L^o(x, \vec{\omega}')(\vec{\omega}' \cdot \vec{n}) d\vec{\omega}', \quad (3)$$

x : Surface point
$\vec{n}$: Unit vector of surface normal at x
$\vec{\omega}$: Direction of outgoing radiance
$\vec{\omega}'$: Direction of incoming radiance
$d\vec{\omega}$: Differential solid angle
Ω : Hemisphere of directions

where L^e, L^r, L^o and f are emitted radiance, reflected radiance, incoming radiance, and a BRDF (i.e. the Torrance-Sparrow model), respectively. Note that the outgoing radiance L is equivalent to the reflected radiance L^r due to the assumption that the object has no emission.

Equations (2) and (3) are theoretical models. The color $\widehat{i_x}$ at a surface point x is represented by the following equation obtained from Eq. (1) [9].

$$\widehat{i_x} = I_x\{\frac{P_{dx}}{\pi} + P_{sx}K(\theta_{vx}, \theta_{rx}, \sigma_x)\}, \quad (4)$$

where I_x is the incoming radiance. $K(\theta_{vx}, \theta_{rx}, \sigma_x)$ denotes the specular term in Eq. (1), and other parameters are the same as in Eq. (1). I_x is decided by counting the number of photons which arrive at the point x. Photons are traced using a Monte Carlo ray tracing method [4]. In this case, the photon is reflected or absorbed depending on the reflectance parameters, and only the photons that are reflected are traced iteratively.

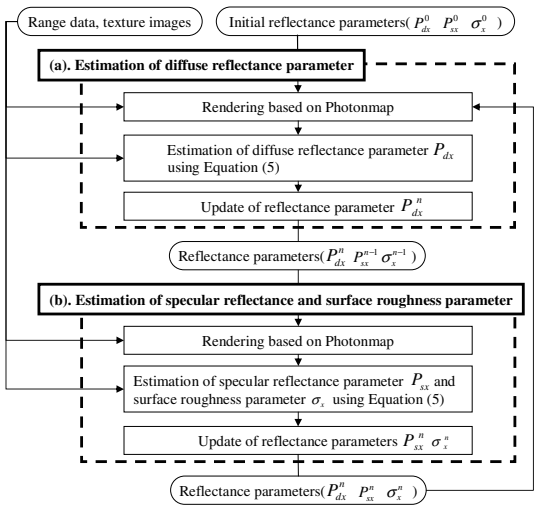

Figure 3. Detail of reflectance estimation process based on photonmap

2.2.2 Iterative estimation of reflectance parameters

Figure 3 details the iterative reflectance estimation process shown in Figure 1 (E). Our approach uses the photon mapping method. The reflectance parameter estimation method based on photon mapping is separated into two processes (a) and (b), as shown in Figure 3. These processes are conducted iteratively. In each process, we minimize the following equation derived from Eq. (4) at each pixel in the texture image.

$$E(P_{dx}, P_{sx}, \sigma_x) = \sum_{j=1}^{q} (i_{xj} - \widehat{i_{xj}})^2, \quad (5)$$

where i_{xj} is the measured radiance (color intensity) and $\widehat{i_{xj}}$ is the irradiance computed from Eq. (4) at the surface point x for light source position j. Here, q denotes the number of sample points.

In process (a), the diffuse reflectance parameter P_{dx}^n is estimated using a T_{diff} pixel. P_{dx}^0, P_{sx}^0 and σ_x^0 are used to compute $\widehat{i_{xj}}$ only at the first iteration. Here, the specular reflection term in Eq. (4), $I_x P_{sx} K(\theta_{vx}, \theta_{rx}, \sigma_x)$, is set to be 0 because the specular reflection can not be observed.

In process (b), the specular reflectance P_{sx}^n and the surface roughness σ_x^n parameters are estimated using only pixels categorized as T_{spec} or T_{none}. Again, P_{sx}^0 and σ_x^0 are used to compute $\widehat{i_{xj}}$ only at the first iteration. P_{dx}^n estimated above is used in Eq. (4). When P_{sx}^n and σ_x^n are estimated, the value of each reflectance parameter is updated and processes (a) and (b) are iterated until $E(P_{dx}, P_{sx}, \sigma_x)$ falls below a threshold th.

3 Experiments

A conventional PC (Pentium 4 3.06 GHz, memory: 2 GB) is used in the following experiments. The number of photons is 2 million and our algorithm requires approximately 4 hours to estimate the reflectance parameters of each object.

As a preliminary experiment, we used Object A (Figure 4(a)), and compared the proposed method to the conventional method I (which does not consider interreflections) [6] and II (which considers only diffuse interreflections) [7]. Object A consists of two plates (region α and β) that are positioned orthogonally to one another and have the same glossy reflectance properties. The results of the comparison are shown in Figure 5. Each graph represents the RGB channels of the diffuse reflectance parameter estimated by one of the three methods. The horizontal axis represents the position of the pixel along the vertical direction of the object, and the vertical axis represents the average of the diffuse reflectance parameters along the horizontal direction of the object. In both conventional methods I and II, the diffuse reflectance parameter is large near the boundary between regions α and β due to the effect of interreflections. In contrast, the parameter estimated using the proposed method, is more stable.

In the next experiment, we use Objects B and C shown in Figures 4(b) and (c). These objects have non-uniform diffuse and specular reflectance properties. Figure 4(d) shows the measurability of both reflection components and the number of selected light sources. The number of selected light sources for estimating the diffuse reflectance parameter is given in brackets. Figure 6 shows real images and differences between real and synthetic cylindrical images (rendered by photon mapping) for the conventional method II and the proposed method. The light position is above the rangefinder. The synthetic images were rendered using the reflectance parameters estimated under the same illumination conditions as those for the real images. Note that linear interpolation is conducted when the specular reflectance and the surface roughness parameters can not be estimated due to their small specular reflection. In the conventional method, the error due to the influence of specular interreflections is confirmed. In particular, Objects B and C have large errors at inequalities (i.e. at the cat's leg and neck and at the pig's nose). The proposed method does not have such a disadvantage. In addition, Table 1 shows the average and variance of differences between real and synthetic images. The proposed method provides an image that is much closer to the real image, compared to the conventional method.

4 Conclusions

In the present paper, we have proposed a new method for densely estimating the non-uniform reflectance properties of real objects based on the global rendering technique. In future research, we intend to reduce the computational cost

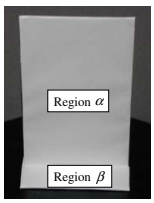

(a) Object A

(b) Object B

(c) Object C

Object	B	C
Light	10(3)	9(3)
Diffuse	100.0%	100.0%
Specular	89.2%	94.7%

(d) Measurability

Figure 4. Three objects used in experiments and measurability of two reflection components

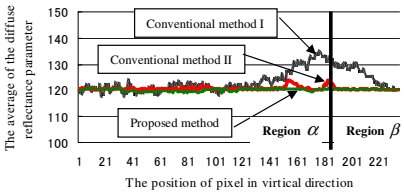

(a) R channel

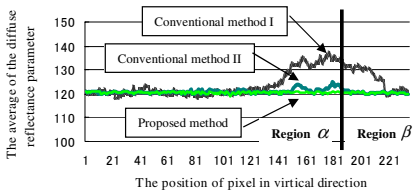

(b) G channel

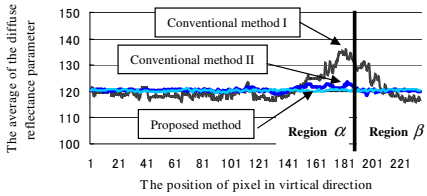

(c) B channel

Figure 5. Comparison with previous research conducted in a preliminary experiment

(a) Real image

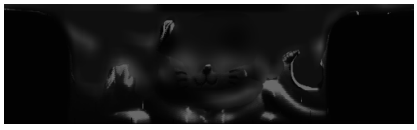

(b) Difference between real and synthetic images in the conventional method II

(c) Difference between real and synthetic images in the proposed method

(d) Real image

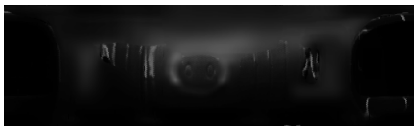

(e) Difference between real and synthetic images in the conventional method II

(f) Difference between real and synthetic images in the proposed method

Figure 6. Differences between real and synthetic cylindrical images for Objects B and C

Table 1. Average and variance of differences between real and synthetic images

		Object B	Object C
Average	Conventional method II	8.7	13.3
	Proposed method	0.51	0.92
Variance	Conventional method II	493.3	375.2
	Proposed method	3.2	9.8

by using a GPU and to synthesize a virtualized object into a real world in real-time.

References

[1] S. Boivin and A. Gagalowicz. Image-based rendering of diffuse, specular and glossy surfaces from a single image. *Proc. SIGGRAPH '01*, pages 107–116, August 2001.

[2] P. Debevec. Rendering synthetic objects into real scenes: Bridging traditional and image-based graphics with global illumination and high dynamic range photography. *Proc. SIGGRAPH '98*, pages 189–198, 1998.

[3] H. W. Jensen. *Realistic Image Synthesis Using Photon Mapping*. A K Peters, Ltd, 1st edition, 2001.

[4] J. T. Kajiya. The rendering equation. *Proc. SIGGRAPH '86*, pages 143–150, August 1986.

[5] C. Loscos, G. Drettakis, and L. Robert. Interactive virtual relighting of real scenes. *IEEE Trans. Visualization and Computer Graphics*, 6(4):289–305, December 2000.

[6] T. Machida, H. Takemura, and N. Yokoya. Dense estimation of surface reflectance properties for merging virtualized objects into real images. *Proc. ACCV 2002*, pages 688–693, January 2002.

[7] T. Machida, N. Yokoya, and H. Takemura. Surface reflectance modeling of real objects with interrefletions. *Proc. 9th Int. Conf. on Computer Vision*, pages 170–177, October 2003.

[8] K. E. Torrance and E. M. Sparrow. Theory for off-specular reflection from roughened surfaces. *Journal of Optical Society of America*, 57(9):1105–1114, 1967.

[9] G. J. Ward. Measuring and modeling anisotropic reflection. *Proc. SIGGRAPH '92*, pages 265–272, July 1992.

[10] Y. Yu, P. E. Debevec, J. Malik, and T. Hawkins. Inverse global illumination: Recovering reflectance models of real scenes from photographs. *Proc. SIGGRAPH '99*, pages 215–227, August 1999.